



Research article

Applying the Hollomon-Jaffe parameter to predict changes in mechanical properties of irradiated austenitic chromium-nickel steels during isothermal exposure

Yerbolat Koyanbayev*

Institute of Atomic Energy Branch of National Nuclear Center of the Republic of Kazakhstan, Kurchatov 071100, Kazakhstan

* **Correspondence:** Email: erbol@nnc.kz; Tel: +7-705-443-9110.

Abstract: The Hollomon-Jaffe parameter is widely used in metallurgy and materials science to characterize the behavior and predict the various metals' physical-mechanical properties under different temperature and time modes. The possibility of predicting changes in the mechanical properties of structural steels due to thermal influences has been studied. The paper presents the results of a study of the mechanical properties of the materials of the core components of the BN-350 reactor facility (RF) made of austenite chromium-nickel steel 12Cr18Ni10Ti (a spent fuel assembly's jacket) and 09Cr16Ni15M3Nb (an intro-channel displacer). The samples were studied both before and after radiation annealing. Annealing of steel samples at 550 °C reduced the yield strength and significantly restored the plasticity and ability of the material to strain hardening. The efficiency of post-radiation annealing of the materials increases with annealing temperature and leads to a transition to the reduction process. It was established that medium of high temperature annealing during heat treatment does not lead to significant changes in the mechanical properties of irradiated materials. The microstructure studied using a scanning electron microscope reasonably correlates with the results of mechanical tests. The possibility of using the Hollomon-Jaffe parameter to predict the properties of austenite chromium-nickel steel, which received damaging doses in the range from 12 to 59 dpa, was shown for the first time. Thus, for the first time, the unique coefficient (C) of the Holloman-Jaffe parameter for irradiated materials of chromium-nickel steel was experimentally determined, and dependencies characterizing the change in hardness of chromium-nickel steel on temperature and duration of post-radiation thermal exposure were established.

Keywords: reactor irradiation; damaging dose; austenite chromium-nickel steel; mechanical properties; post-radiation annealing; BN-350 reactor facility; Hollomon-Jaffe parameter

1. Introduction

Structural materials of fuel assemblies (FAs), in general, and fuel rods, in particular, must maintain integrity and strength during the entire period of operation of a nuclear facility (NF) and the subsequent period of “wet” and long-term “dry” storage of spent fuel assemblies (SFA), while ensuring reliable retention of fission products inside the fuel rod. Knowledge of the mechanisms and kinetics of radiation and thermal damage leading to degradation of structural materials properties is essential for making important decisions regarding the use of these materials in the design of nuclear units, life extension, and decommissioning, as well as in justifying the safety of nuclear units at all stages of the life cycle, including the stage of spent nuclear fuel (SNF) management.

Even though certain successes have been achieved in the field of studies of radiation-induced changes in austenite steels, such important problems as the evolution of radiation-induced structure and the physical and mechanical properties of irradiated structural steels under conditions of intensive external influence of natural and thermal aging factors on them remain practically undisclosed. The number of publications in this area is limited, although the results of such studies are of undeniable scientific and practical interest, especially regarding the structural materials of fast reactors.

Special attention towards these reactors’ steels is conditioned by the fact that they undergo thermo-mechanical annealing before use, not excluding direct and reverse martensite transformations, which can influence swelling and other strength and structural properties of steels.

It is also well known that as radiation damage accumulates, structural steel’s phase and structural states change and radiation effects such as swelling, creeping, and embrittlement develop, leading to the material’s mechanical properties deteriorating and a reduction in their service life. Long-term annealing makes it possible to restore the mechanical properties of steels by thermally induced removal of the products of radiation damage [1–10].

Despite the knowledge gained in structural-phase transformations and restoration of mechanical properties due to thermal effects, the issue of predicting changes in the operational properties of materials during long-term wet and dry storage of SFA from power reactors remains relevant [11].

In metallurgy, it is a common practice to describe the behavior and predict the properties of the metallic materials under various temperature and time modes using the Hollomon-Jaffe (HJ) parameter [12,13]. The effect of tempering temperature and exposure time on the steel properties is considered in [14], and the assessment of the erosion-resistant steel durability is completed in [15]. Applying the HJ parameter to the structural steels after their operation in the reactor, whose structure and properties changed depending on temperature, time, damaging doses, and rate, is possible under the condition of experimental determination of the equation parameter.

The ultimate goal of the investigation was to establish the regularities of change in strength properties of irradiated austenite steel samples from temperature and duration of post-radiation thermal impacts. This objective is conditioned by the necessity to improve the validity of the SFA materials condition evaluation and develop guidelines for managing the SFA storage packs (containers) of the BN-350 RF following 50 years of dry storage.

2. Materials and methods

The object of the investigations were samples of austenite steels of grades 12Cr18Ni10Ti that were cut from the fuel assembly casing walls and 09Cr16Ni15M3Nb that were cut from the intro-channel displacers of the BN-350 reactor facility (RF). The samples were exposed to radiation at doses ranging from 12 to 59 dpa. The selection of these steels is influenced by two factors: the radiation embrittlement effect in the fuel assembly casings, which results in a loss of ductility; and the proximity of the intro-channel displacer's composition to the fuel element cladding composition, positioned as the first barrier on the way fission products release from the reactor facility into the medium. Tables 1 and 2 provide information on the chemical composition of steels and their irradiation parameters.

Table 1. Chemical composition of the steels, wt.%.

Material	Fe	C	Cr	Ni	Ti	Si	Mn	Mo	Nb	P	S
12Cr18Ni10Ti	Base	0.12	17.00	10.66	0.50	0.80	1.67	0.00	0.00	0.03	0.00
09Cr16Ni15M3Nb		0.09	16.00	15.00	0.00	0.80	0.80	3.00	0.90	0.03	0.02

Table 2. Irradiation parameters of the research samples.

No.	Material	Irradiation dose, dpa	Rate of gain in dose, 10 ⁻⁶ dpa/s	Operating time, days	Irradiation temperature, °C
1	12Cr18Ni10Ti	12.30	0.04	3696.70	350.00
2	(SFA jacket)	17.00	0.31	643.80	350.00
3		28.70	0.62	537.60	350.00
4		45.00	1.40	370.90	300.00
5		45.50	1.42	370.90	410.00
6		48.20	1.91	291.80	350.00
7		50.00	1.56	370.90	310.00
8		50.50	1.58		390.00
9		55.50	1.73		375.00
10		58.90	1.84		350.00
11	09Cr16Ni15M3Nb	47.70	1.71	323.20	320.00
12	(intro-channel	50.50	1.81		350.00
13	displacer)	48.00	1.72		375.00

To conduct long-term thermal tests and determine the mechanical properties, micro-samples with a reduced cross-section of the working part were made. The micro-samples for testing were made using the electro-erosion method. Figure 1 shows the sizes of the micro-sample and its appearance.

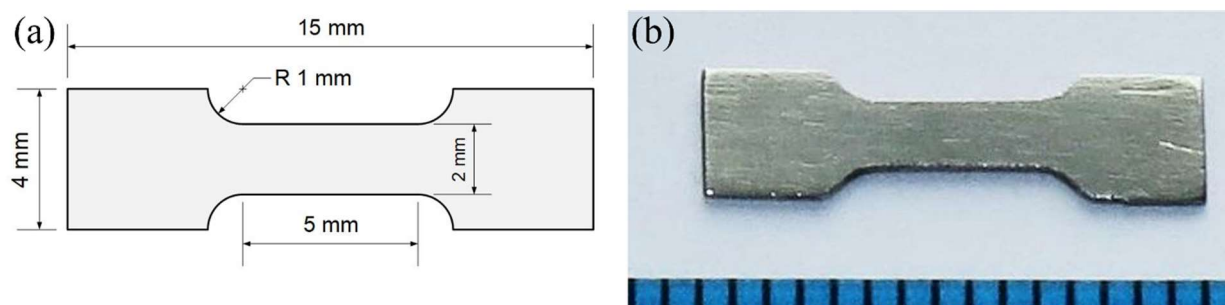


Figure 1. Micro-sample for mechanical and thermal tests: (a) micro-sample design and (b) micro-sample's appearance.

Testing the samples of BN-350 RF structural materials was carried out in a SNOL-8,2/1100 electric muffle furnace, equipped with a chrome-alumini thermocouple at temperatures of 300, 400, 450, 550, and 600 °C in air and an argon medium. The set temperature in the operating chamber of the furnace with an accuracy of ± 2 °C was carried out and maintained by the built-in OMRON E5CN controller.

The material science research on the samples was conducted to obtain data on the degree of change in the structure and the physical and mechanical properties of the structural materials of BN-350 RF SFA depending on the received dose of the reactor irradiation and subsequent conditions of the thermal tests.

The metallographic studies of the irradiated samples were performed using Metam LV-41 and ICX41M optical microscopes. The electron microscopic studies of the material were carried out using a Tescan Vega 3 LMH scanning electron microscope in the secondary electron mode. X-ray spectral microanalysis by an Oxford Ins. X-Act energy dispersion spectrometer was used for a qualitative assessment of the content and distribution of the elements.

Mechanical tests of the samples included the determination of hardness, as well as the strength characteristics of the samples. The strength characteristics were determined by the uniaxial stretching method on the Instron 5966 universal testing machine. The tests were performed at room temperature with a deformation rate of 2.5 mm/min. The self-centered grips without clamping were used [16] to hold the micro-sample, designed in the IAE NNC RK [17–20]. The grips include an active and passive half-grip and a cell for a micro-sample. To exclude the rotation and displacement of the micro sample axis, the gripper is equipped with the cylindrical guides installed in the graphite bushings (Figure 2). The strain value of the test sample was recorded with an AVE-2 video tensiometer (Instron) during the movement of the machine traverse. The hardness was determined on the sections prepared for the metallographic studies using an automatic micro-hardness tester (Qness Q10A+) according to the Vickers scheme with an indenter load of 200 g.

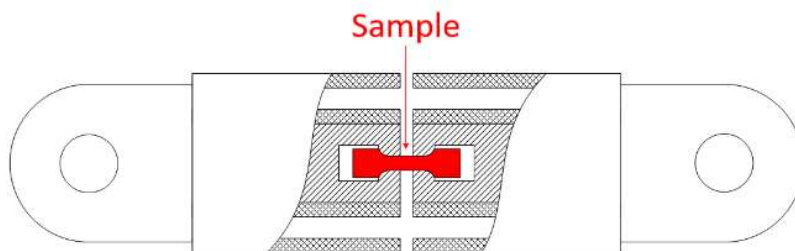


Figure 2. Self-centering grip.

3. Results and discussion

3.1. Characterization of the material after reactor irradiation

To characterize the state of materials after operation in the BN-350 RF, comprehensive studies of irradiated materials were conducted [21–25]. Microstructural studies of the samples after thermal tests at 550 °C in argon medium revealed that the structure of the samples is homogeneous and has a polyhedral structure of austenite. In the grain body of the irradiated sample, there are numerous finely dispersed carbides, whereas in the non-irradiated sample, such carbides are practically absent (Figure 3).

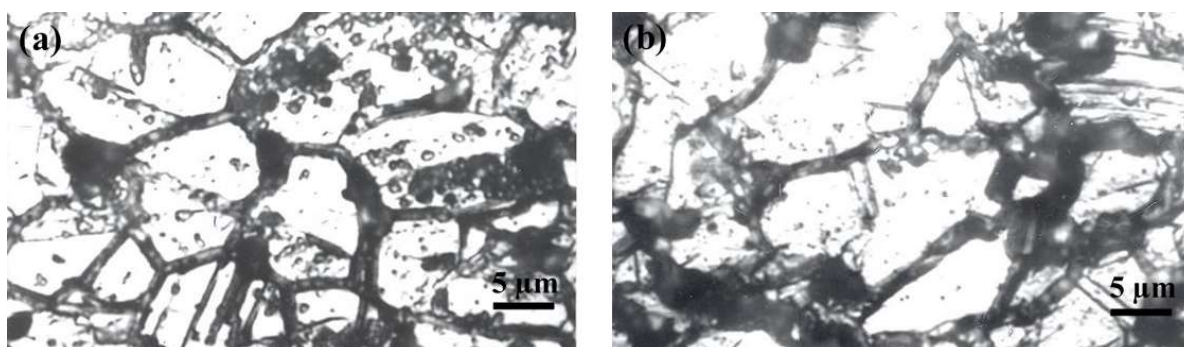


Figure 3. Microstructure of 12Cr18Ni10Ti steel sample after long-term annealing at 550 °C for 7000 h: (a) non-irradiated sample and (b) irradiated sample.

To determine the composition of dispersed separations, local elemental analysis was performed with the plotting of distribution maps of the elements (Figure 4). The element distribution maps show that in the structure of steel, besides titanium, there are also chromium and nickel carbides.

According to the obtained results, the corrosion damage to both non-irradiated and neutron-irradiated samples was mainly of an intercrystalline nature. A decrease in resistance to corrosion cracking after neutron irradiation of the considered steels is noted in [15,16,21].

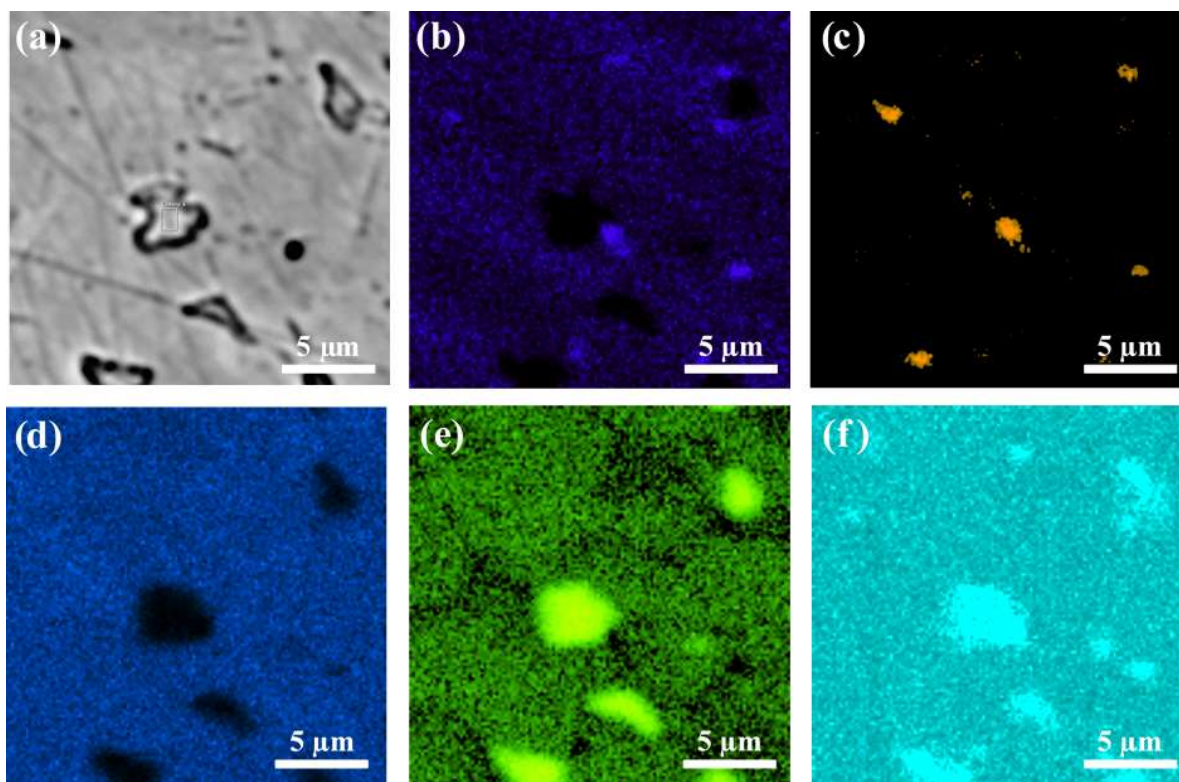


Figure 4. Results of the elements' spatial distribution in the SFA jacket sample: (a) investigated region; (b) mapping for Ni; (c) mapping for Ti; (d) mapping for Fe; (e) mapping for Cr and (f) mapping for C.

It has been established that the penetration depth of intercrystalline corrosion on the wall inner surface is higher than on the wall outer surface of the SFA jacket and increases with the increasing values of the damaging doses (Figure 5). The dependence of the corrosion destruction of the material surface on the irradiation dose has been established based on the analysis of the obtained experimental data.

The obtained dependencies allow for estimating the depth of penetration of inter-granular corrosion on the SFA walls and will be very useful in estimating the allowable loads during SFA handling, taking into account the remaining wall thickness.

According to the measurement results, after irradiation, the steel samples had increased surface hardness due to the presence of radiation defects in the structure [2,11,26–28]. The measurements revealed a slight difference in the micro-hardness values for the samples, with radiation doses varying in the range of 12–58.9 dpa (Figure 6). This is consistent with known literature data and is explained by the saturation effect of the steel radiation hardening after overcoming the conditional threshold value of the radiation dose of 2–5 dpa [29].

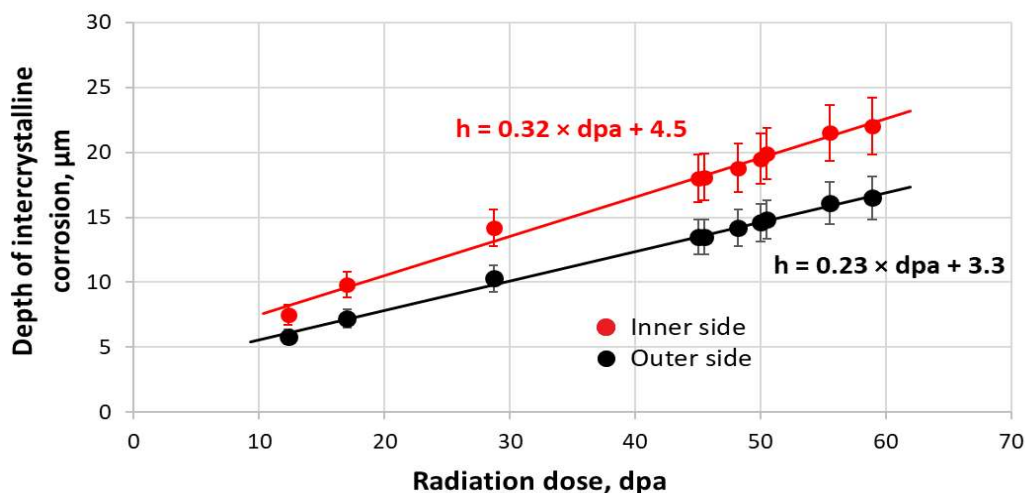


Figure 5. Penetration depth of the intercrystalline corrosion on the outer and inner walls of the SFA depending on the damaging doses.

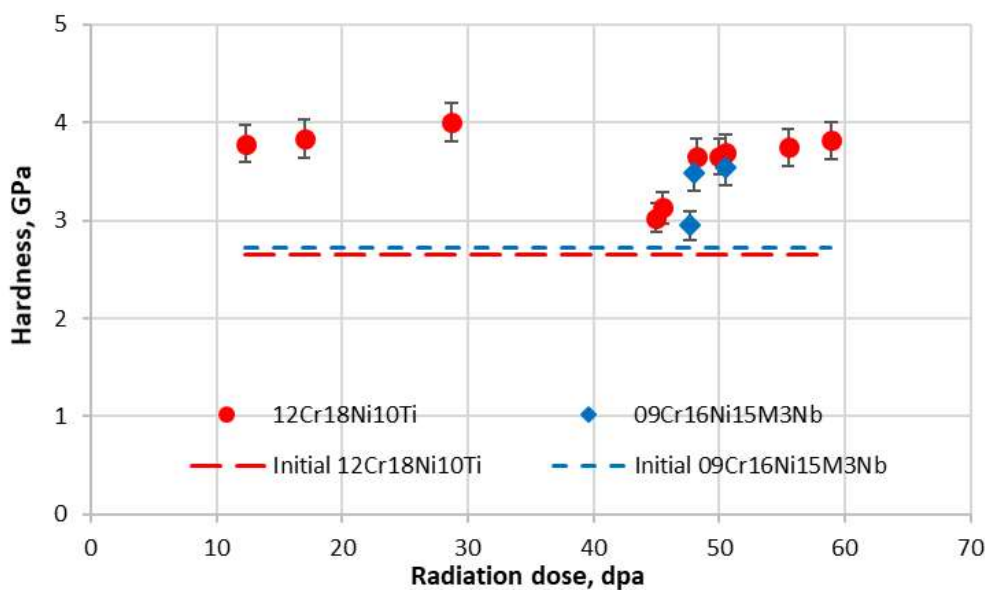


Figure 6. Hardness dependence on the damaging dose.

3.2. Structure and properties of the material after thermal testing

To conduct the comparative studies of the mechanical properties of the SFA jacket material after thermal tests, the strength characteristics of the samples subjected to isothermal annealing for 7000 h at temperatures of 300, 400, and 550 °C have been determined. Figure 7 shows stretching test results as a diagram of deformations in σ – ε coordinates. The experiments were carried out until the destruction of each of the micro-samples.

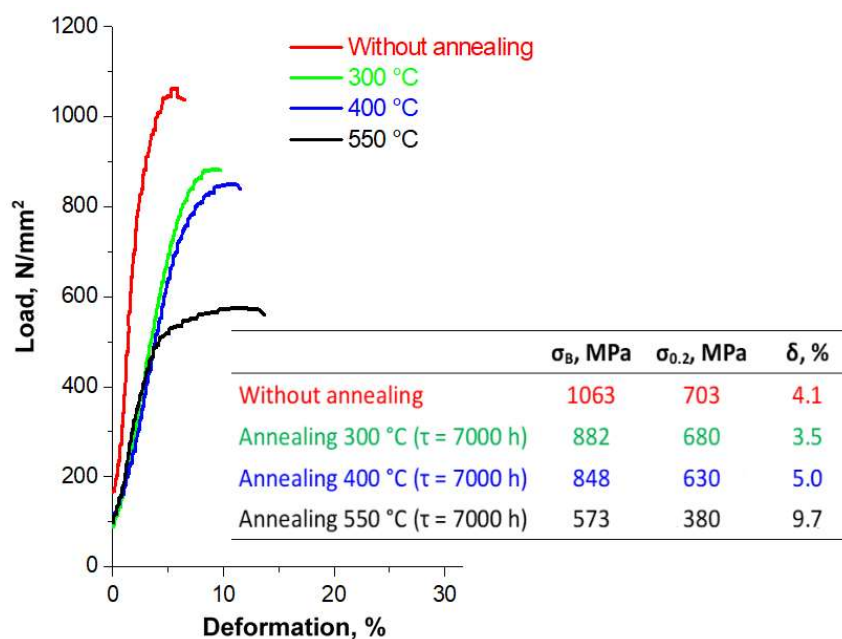


Figure 7. Stretching diagram of highly irradiated samples.

According to the type of stretching diagrams obtained, the micro-samples, both in the initial state and after the thermal annealing, can be attributed to the materials that do not have a yield point but are slightly deformed under load, that is, brittle.

From the study of the strength characteristics of the micro-samples of the SFA jacket of the BN-350 material in the initial state (after the reactor irradiation) and thermal tests, we draw the following observations (Figure 7):

- Reactor irradiation has resulted in the significant strengthening of the studied micro-samples (the increasing of the strength characteristics depends on the irradiation dose compared with the initial ones) [29,30].
- The decrease in the radiation hardening after the thermal tests is presumably due to the partial annealing of the radiation defects.

At the same time, as Figure 7 shows, a sharp decrease (55%) in the strength characteristics of the samples is observed at an annealing temperature of 550 °C. According to [31,32], the steel heating above the irradiation temperature increases the diffusion mobility of the point defects, which is a prerequisite for the appearance of the thermodynamic instability of various radiation defects in the steel and, thus, creates the conditions for the restoration of mechanical properties. Since the annealing process of the irradiated samples is accompanied by the recombination of the point defects, there is a decrease in the density of the linear dislocations, dislocation loops, and pores, as well as a decrease in the density and an increase in the size of the radiation-induced secondary phase emissions, which subsequently results in a decrease in the temperature of the visco-brittle transition and an increase in the material plasticity [33,34].

As Figure 7 shows, the irradiation has led to an increase in the steel's strength characteristics. The presented dependencies show that an increase in the test temperature of the irradiated steel from room temperature to 550 °C has led to a decrease in the mechanical characteristics. As can be seen in Figure 7, the plasticity, characterized by the δ relative elongation, will increase along with the test temperature.

At the same time, at temperatures of 300 and 400 °C, it is also possible to achieve a similar recovery nature, but this requires a significant increase in the process duration significantly [35,36].

It should be considered that prior to placement in the reactor, 12Cr18Ni10Ti steel was subjected to a thermo-mechanical treatment consisting of 20% cold deformation followed by annealing at 800 °C for 1 h. In this case, the nominal yield strength $\sigma_{0.2}$ corresponds to 310–330 MPa and the nominal tensile strength $\sigma_B \sim 650$ –700 MPa.

The effect of softening the irradiated steel samples after the thermal tests is also confirmed by the results of the hardness determination (Figure 8). As the results show, the values of the yield strength and time resistance of the samples converge depending on the temperature of the thermal effect. According to the obtained results, even if the measurement results are within an error margin, the following point can be noted: the results of measuring the hardness of the samples cut from the assemblies of the central casing 48 and 59 dpa are grouped and are at the error lower limit, while the results of the samples cut from the assemblies of the screen casings 12, 17, and 29 dpa are grouped and are at the upper limit of the error limit.

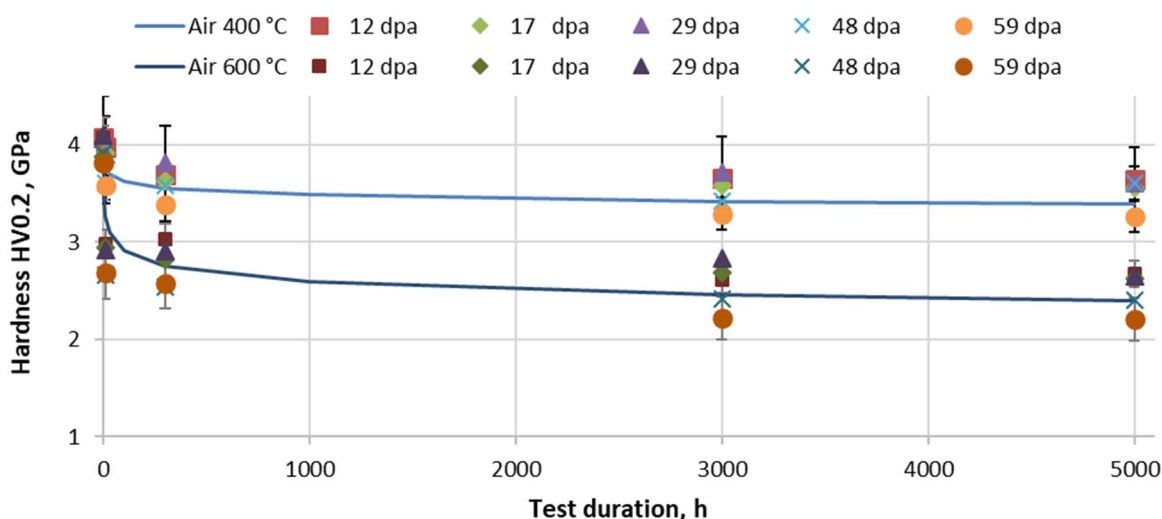


Figure 8. Change in the hardness of samples depending on the duration of tests.

However, Figure 9 shows the results of measuring the micro-hardness of the irradiated samples after thermal exposure, which are practically identical. This indicates that the annealing medium, even with a test duration of 5000 h, practically does not affect the change in the properties of the samples.

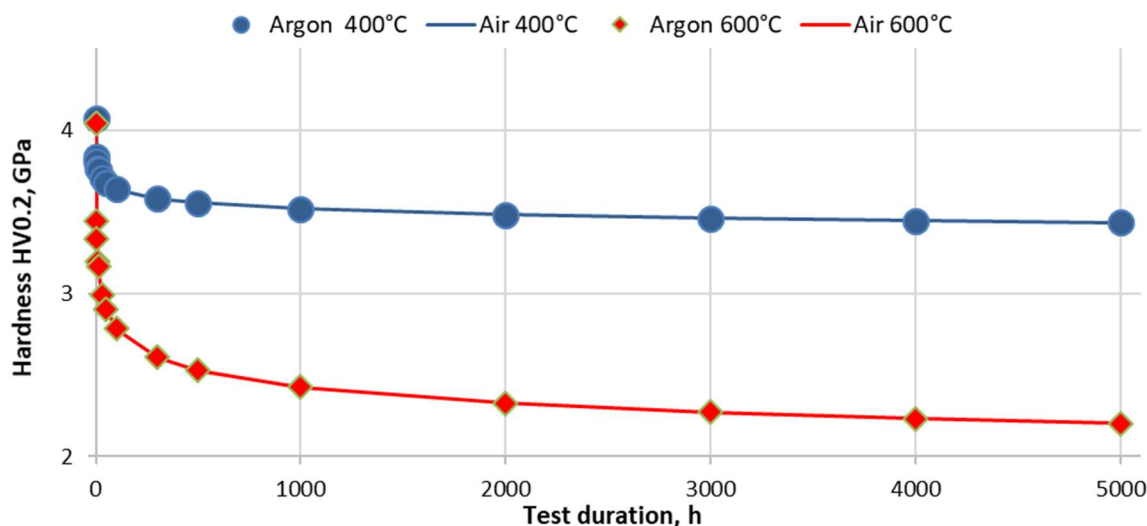


Figure 9. Change in the hardness of the samples depending on the medium of the thermal exposure (markers denote the hardness values of samples tested in argon medium, and the lines denote in air medium).

3.3. Prediction of changes in the hardness of the irradiated material depending on the duration and temperature of the test

To assess the possibility of predicting the long-term properties of the irradiated material, the HJ equation [11–15] has been used, describing the relationship between the test temperature and the exposure time, which allows predicting the kinetics of changes in the micro-hardness of the samples of the SFA casing material at various temperature-time parameters, defined by Eq 1:

$$(TP) = T \times (C + \log \tau) \quad (1)$$

where TP is the HJ parameter, T is temperature (K), τ is exposure time (h), and C is constant, depending on the material properties.

According to Eq 1, with the same HJ parameter, the properties of the studied material obtained under different temperature-time modes coincide, that is, in the future, the necessary properties can be obtained by varying the temperature and exposure time in accordance with the Eq 1. To assess the effect of the process parameters on the material properties, it is necessary to know the value of the constant C . According to [37], the value of C for the structural steels is equal to 20. However, in our case, in the initial state, the samples of 12Cr18Ni10Ti steel cut from regular SFA have been considered; during operation, they received damaging doses in the range of 12–59 dpa. Therefore, this parameter has been determined from the experimental data by the Eq 2:

$$C = \frac{T_2 \log \tau_2 - T_1 \log \tau_1}{T_1 - T_2} \quad (2)$$

where multiplications $T_2 \log \tau_2$ and $T_1 \log \tau_1$ correspond to two temperature-time modes, ensuring the same material properties. The hardness values of the samples exposed to two distinct temperature-time exposures are equal, which suggests that the HJ parameter is also comparable.

After 3 h annealing at 600 °C, the micro-hardness of structural steel (SS) is 3.44 GPa. According to the graph, the same hardness is achieved after 4000 h annealing at 400 °C (Figure 10). Thus, the equality of the hardness values of the samples subjected to two different temperature-time exposures indicates the equality of the HJ parameter, which allows determining the value of the constant C by solving Eq 2. For $T_1 = 600$ °C, $\tau_1 = 3$ h and $T_2 = 400$ °C, $\tau_2 = 400$ h, where the value of C is 10.

Having obtained the values for T_2 , τ_2 from the graphical dependence, the work has been carried out to check the value of $C = 10$ for the compliance with the known experimental data obtained using direct measurements that were done during unloading the samples at the control points. Figure 10 shows the obtained results, which coincided with the micro-hardness values, that is, the deviation from the values obtained during the test durations of 10 and 5000 h was less than 1.5%.

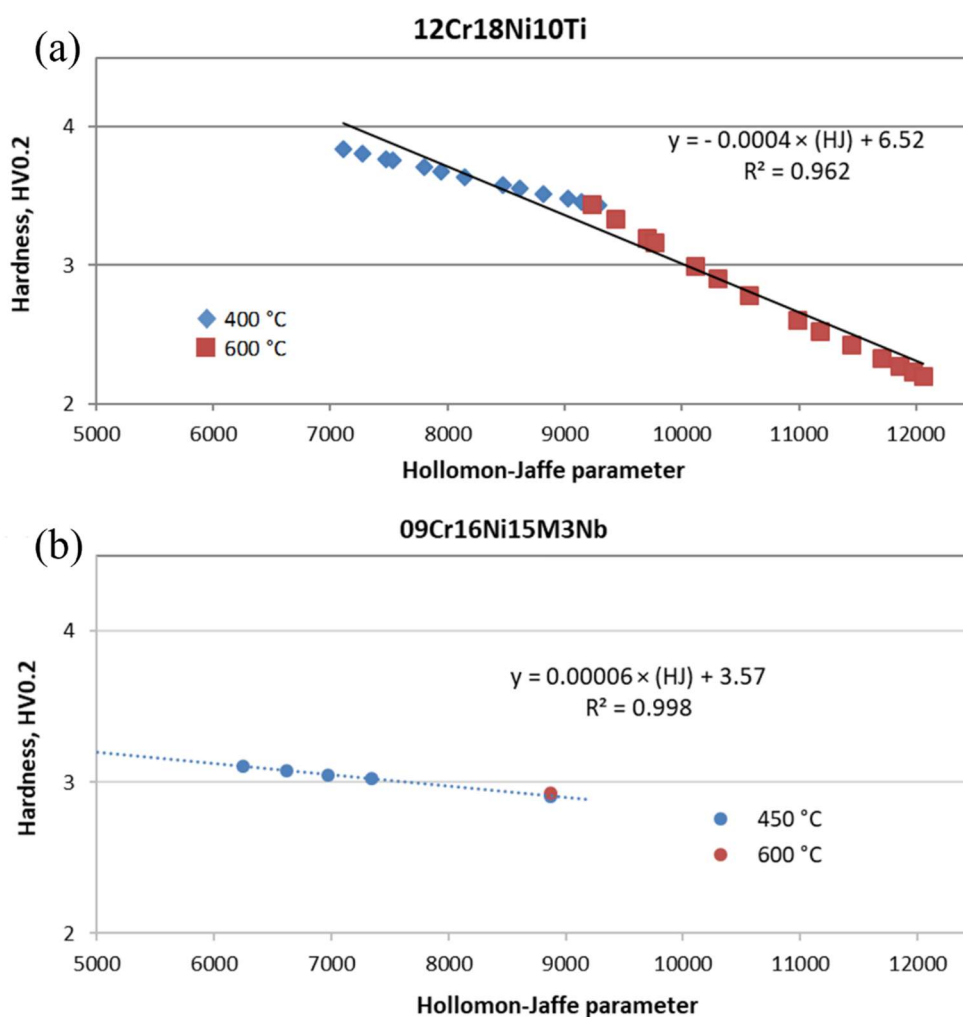


Figure 10. Diagram of dependence of hardness for (a) 12Cr18Ni10Ti and (b) 09Cr16Ni15M3Nb on HJ parameter during the isothermal tests.

Similarly, the dependence of the change in the hardness of the irradiated samples of 09Cr16Ni15M3Nb chromium-nickel steel was determined (Figure 10). Thus, the dependence of the change in radiation-induced hardness on the temperature and duration of the test has the following form:

- For steel 12Cr18Ni10Ti–HV = 6.52 – 0.0004 × T × (10 + log(τ));
- For steel 09Cr16Ni15M3Nb–HV = 3.57 – 0.00006 × T × (10 + log(τ)).

4. Conclusions

The possibilities of restoring the structural, phase state and mechanical properties of 12Cr18Ni10Ti and 09Cr16Ni15M3Nb structural steels by means of annealing at different parameters have been studied. It was established that thermal tests lead to softening of the material, which is due to partial annealing of radiation defects. The softening depends on the irradiation conditions and the test temperature. At the same time, the test medium contributes to the softening only at the initial time. The efficiency of restoring the critical brittleness temperature increases with an increase in the annealing temperature, and the process of restoring the initial characteristics is more efficient.

An approach has been developed to forecast the properties of the irradiated austenite chromium-nickel steel under the conditions of long-term temperature exposure using the HJ parameter. The coefficient *C* of the HJ parameter for the irradiated chromium-nickel steel with damaging doses in the range of 12–59 dpa has been experimentally determined. The comparison with the measurement data of the hardness value confirmed the correctness of determining the coefficient for the samples under study. As a result, the dependencies that describe the change in the hardness of chromium-nickel steel on temperature and duration of the post-radiation thermal exposure were established, which makes it possible to forecast the evolution of the mechanical properties of the construction materials during long-term dry storage of SNF in the power reactors. The research results will be used to forecast the parameters of BN-350 SFAs during long-term storage and to determine the strategy for their further handling.

Use of AI tools declaration

The author declares that no Artificial Intelligence (AI) tools were used in the creation of this article.

Acknowledgments

This research was funded by the Science Committee of the Ministry of Science and Higher Education of the Republic of Kazakhstan within the framework of the scientific and technical program “Research to support the creation and safe operation of a nuclear power plant in the Republic of Kazakhstan” (IRN - BR21882185).

Conflict of interest

The author declares no conflict of interest.

References

1. Skakov MK, Melikhov VD (2001) Specific features of radiation inheritance. *Russ Phys J* 44: 608–612. <https://doi.org/10.1023/A:1012543812065>
2. Xiao X (2019) Fundamental mechanisms for irradiation-hardening and embrittlement: A review. *Metals* 9: 1132. <https://doi.org/10.3390/met9101132>

3. Cole JI, Allen TR (2000) Microstructural changes induced by post-irradiation annealing of neutron-irradiated austenitic stainless steels. *J Nucl Mater* 283–287: 329–333. [https://doi.org/10.1016/S0022-3115\(00\)00072-6](https://doi.org/10.1016/S0022-3115(00)00072-6)
4. Kascheev VA, Shadrin AYu, Dmitriev SA (2020) Optimization of RW volumes from reprocessing of SNF from fast reactors. Fractionation options. *J Phys Conf Ser* 1475: 012023. <https://doi.org/10.1088/1742-6596/1475/1/012023>
5. Mitskevich AV (2015) Development of neutron spectrum analysis method to assess the content of fissile isotopes in SFA. *Nucl Eng Technol* 1: 202–207. <https://doi.org/10.1016/j.nucet.2016.02.001>
6. Podgornov VA (2014) Implementation of automated process control systems for SNF handling. *NRNU MEPhI* 11: 532–537.
7. Dikov AS, Chernov II, Kislitsin SB (2018) Influence of the test temperature on the creep rate of 0.12C18Cr10NiTi structural steel irradiated in the BN-350 reactor. *Inorg Mater Appl Res* 9: 357–360. <https://doi.org/10.1134/S2075113318030127>
8. Kuleshova EA, Fedotov IV, Maltsev DA, et al. (2022) Structural features ensuring the increase of service characteristics of high-nickel steels for pressure vessels of prospective energy-generation reactors. *Int J Pres Ves Pip* 200: 104845. <https://doi.org/10.1016/j.ijpvp.2022.104845>
9. Bushuev AV, Kozhin AF, Glagovsky EM (2013) Determination of the residual content of fissile materials in fuel from spent fuel assemblies with high initial enrichment by the active neutron method. *At Energy* 114: 428–432. <https://doi.org/10.1007/s10512-013-9734-7>
10. Bushuev AV, Kozhin AF, Aleeva TB (2016) A setup for active neutron analysis of the fissile material content in fuel assemblies of nuclear reactors. *Phys At Nucl* 79: 1362–1366. <https://doi.org/10.1134/S1063778816080056>
11. Xu C, Chen WY, Zhang X, et al. (2018) Effects of neutron irradiation and post-irradiation annealing on the microstructure of HT-UPS stainless steel. *J Nucl Mater* 507: 188–197. <https://doi.org/10.1016/j.jnucmat.2018.04.043>
12. Sun Y, Obasi G, Hamelin C, et al. (2019) Characterisation and modelling of tempering during multi-pass welding. *J Mater Process Technol* 270: 118–131. <https://doi.org/10.1016/j.jmatprotec.2019.02.015>
13. Virtanen E, Van Tyne CJ, Levy BS, et al. (2013) The tempering parameter for evaluating softening of hot and warm forging die steels. *J Mater Process Technol* 213: 1364–1369. <https://doi.org/10.1016/j.jmatprotec.2013.03.003>
14. Liu G, Yang S, Han W, et al. (2018) Microstructural evolution of dissimilar welded joints between reduced-activation ferritic-martensitic steel and 316L stainless steel during the post weld heat treatment. *Mater Sci Eng A* 722: 182–196. <https://doi.org/10.1016/j.msea.2018.03.035>
15. Cheng G, Choi KS, Hu X, et al. (2017) Predicting deformation limits of dual-phase steels under complex loading paths. *JOM* 69: 1046–1051. <https://doi.org/10.1007/s11837-017-2333-7>
16. Baklanov VV, Koyanbaev ET, Skakov MK, et al. (2017) Gripper for fastening of microsamples during tensile testing. Republic of Kazakhstan Patent No. 32305.
17. Gordienko Yu, Ponkratov Yu, Kulsartov T, et al. (2020) Research facilities of IAE NNC RK (Kurchatov) for investigations of tritium interaction with structural materials of fusion reactors. *Fusion Sci Technol* 76: 703–709. <https://doi.org/10.1080/15361055.2020.1777667>

18. Batyrbekov E, Khasenov M, Gordienko Yu, et al. (2022) Experimental facility to study the threshold characteristics of laser action at the p-s-transition of noble gas atom upon excitation by ${}^6\text{Li}(n,\alpha){}^3\text{H}$ nuclear reaction products. *Appl Sci* 12: 12889. <https://doi.org/10.3390/app122412889>
19. Samarkhanov K, Batyrbekov E, Khasenov M, et al. (2019) Study of luminescence in noble gases and binary Kr-Xe mixture excited by the products of ${}^6\text{Li}(n,\alpha)\text{T}$ nuclear reaction. *Eurasian Chem-Technol J* 21: 115–123. <https://doi.org/10.18321/ectj821>
20. Gordienko Yu, Khasenov M, Batyrbekov E, et al. (2018) Luminescence of noble gases and their mixtures under nanosecond electron-beam excitation. *J Appl Spectrosc* 85: 600–604. <https://doi.org/10.1007/s10812-018-0692-7>
21. Koyanbayev YeT, Skakov MK, Batyrbekov EG, et al. (2019) The forecasting of corrosion damage of structural materials during dry long-term storage of RD BN-350 SNF with CC-19 SFA. *Sci Technol Nucl Ins* 2019: 1293060. <https://doi.org/10.1155/2019/1293060>
22. Rofman OV, Maksimkin OP, Koyanbayev YeT, et al. (2018) The natural aging of austenitic stainless steels irradiated with fast neutrons. *J Nucl Mater* 499: 284–293. <https://doi.org/10.1016/j.jnucmat.2017.11.006>
23. Koyanbayev ET, Sitnikov AA, Skakov MK, et al. (2017) Microstructural changes of mechanical properties of 08Cr18Ni10Ti austenitic steel under neutron irradiation. *Key Eng Mater* 743: 37–40. <https://doi.org/10.4028/www.scientific.net/KEM.743.37>
24. Kozhakhmetov YeA, Koyanbayev YeT, Sapatayev Ye, et al. (2019) Study of the change in the physical and mechanical properties of materials of spent FAs of the BN-350 reactor under conditions of long-term thermal aging. *NNC RK Bulletin* 1: 45–51. <https://doi.org/10.52676/1729-7885-2019-1-45-51>
25. Koyanbayev YeT, Skakov MK, Ganovichev DA, et al. (2019) Simulation of the thermal conditions of cask with fuel assemblies of BN-350 reactor for dry storage. *Sci Technol Nucl Ins* 2019: 3045897. <https://doi.org/10.1155/2019/3045897>
26. Busby JT, Hash MC, Was GS (2005) The relationship between hardness and yield stress in irradiated austenitic and ferritic steels. *J Nucl Mater* 336: 267–278. <https://doi.org/10.1016/j.jnucmat.2004.09.024>
27. Larionov AS, Dikov AS, Poltavtseva VP, et al. (2015) Radiation thermal processes in Cr13Mo2NbVB steel—The material of the fuel assembly shell in reactor BN-350 under mechanical tests. *IOP Conf Ser Mater Sci Eng* 81: 012035. <https://doi.org/10.1088/1757-899X/81/1/012035>
28. Tsai KV, Maksimkin OP, Turubarova LG (2008) Influence of irradiation and post-radiation heat treatment on the microstructure and properties of 12C18N9T steel irradiated in the WWR-K research reactor up to 5 dpa. *Probl At Sci Technol* 92: 100–107.
29. Garner FA (2012) Radiation damage in austenitic steels, In: Konings RJM, *Comprehensive Nuclear Materials*, 2 Eds., Oxford: Academic Press, 33–95.
30. Lucas GE (1993) The evolution of mechanical property change in irradiated austenitic steels. *J Nucl Mater* 206: 287–305. [https://doi.org/10.1016/0022-3115\(93\)90129-M](https://doi.org/10.1016/0022-3115(93)90129-M)
31. Nikolaeva AV, Nikolaev YA, Kevorkyan YR (2001) Restoration of mechanical properties of irradiated steel by thermal annealing. *At Energy* 90: 475–479. <https://doi.org/10.1023/A:1012313210033>

32. Kryukov AM, Nikolaev YuA, Nikolaeva AV (1998) Behavior of mechanical properties of nickel-alloyed reactor pressure vessel steel under neutron irradiation and post-irradiation annealing. *Nucl Eng Des* 186: 353–359. [https://doi.org/10.1016/S0029-5493\(98\)00247-7](https://doi.org/10.1016/S0029-5493(98)00247-7)
33. Tsai KV, Rofman OV, Ostavnov MA (2019) Change in the phase composition and strength properties of austenitic steel 12C18N10T as a result of deformation and post-deformation annealing. *NNC RK Bulletin* 1: 72–78. <https://doi.org/10.52676/1729-7885-2019-1-72-78>
34. Merezhko DA, Gushev MN, Merezhko MS, et al. (2022) Morphology and elemental composition of a new iron-rich ferrite phase in highly irradiated austenitic steel. *Scripta Mater* 215: 114690. <https://doi.org/10.1016/j.scriptamat.2022.114690>
35. Amaev AD, Kryukov AM, Sokolov MA (1993) Recovery of transition temperature of irradiated WWER-440 vessel metal by annealing. *ASTM STP* 25: 369–379. <https://doi.org/10.1520/STP24787S>
36. Merezhko MS, Merezhko DA, Rofman OV (2022) Macro-scale strain localization in highly irradiated stainless steel investigated using digital image correlation. *Acta Mater* 231: 117858. <https://doi.org/10.1016/j.actamat.2022.117858>
37. Golovanov VN, Shamardin VK, Prokhorov VI, et al. (2001) Investigations of BOR-60 structural materials and prospects for further work. *At Energy* 91: 937–950. <https://doi.org/10.1023/A:1014222025196>



AIMS Press

© 2024 the Author(s), licensee AIMS Press. This is an open access article distributed under the terms of the Creative Commons Attribution License (<http://creativecommons.org/licenses/by/4.0>)